MITIGATION OF MEMORY EFFECTS IN BETA SCINTILLATION CELLS FOR RADIOACTIVE GAS DETECTION

Carolyn E. Seifert, Justin I. McIntyre, Kathryn C. Antolick, April J. Carman, M.W. Cooper, James C. Hayes, Tom R. Heimbigner, Charles W. Hubbard, Kevin E. Litke, Mike D. Ripplinger, and Reynold Suarez

Pacific Northwest National Laboratory

Sponsored by National Nuclear Security Administration
Office of Nonproliferation Research and Engineering
Office of Defense Nuclear Nonproliferation

Contract No. DE-AC05-76RL01830

ABSTRACT

Detection of radioactive noble gases can provide definitive evidence of a nuclear explosion at large stand-off distances. The Automated Radioxenon Sampler/Analyzer (ARSA) developed at Pacific Northwest National Laboratory (PNNL) measures the relative concentrations of xenon isotopes using a β-γ coincidence system. Typically, a set of plastic scintillating cells are surrounded by a NaI(Tl) scintillator. The cells are evacuated and the background count rate is measured before the cell is filled with sampled air. Any radioxenon present in the air emits β particles, which are detected in the plastic cell, as well as coincident γ rays, which are detected in the NaI(Tl). When a sample count is finished, the cell is again evacuated, and another background count is taken before measuring the next air sample. Previous tests of the ARSA system have shown that latent radioactivity remains in the plastic cells after evacuation of the gases, leading to a "memory effect" in which the background count rate is dependent on the sample history. The increased background results in lower detection sensitivity.

Two possible solutions to the memory effect are explored in this work: depositing a thin layer of metal on the plastic cell ("metallization"), and using an inorganic scintillating cell composed of yttrium aluminum perovskite (YAP). In both cases, the presence of inorganic material at the surface is intended to inhibit the diffusion of gases into the cell walls.

In the metallization experiments, several different metals (Al, Cu, chrome) were deposited on plastic cells using electron beam lithography. The light collection performance of the cells was evaluated using standard sealed γ-ray sources and compared to a bare plastic cell. The aluminized cell demonstrated comparable light collection performance and good adhesion to the plastic and was chosen for further studies.

The aluminized cell, YAP cell, and bare plastic cell were each placed in the void of a CsI(Na) well counter and injected with radioactive xenon and radon. β-γ coincidence measurements were taken before, during, and after injection of radioactive gases. The YAP cell demonstrated little or no observable memory effect, while the aluminum-coated plastic cell showed reduced latent radioactivity relative to the bare cell as expected. Although the memory effect results for the YAP cell are promising, the wall thickness is too large for the escape of the xenon x-rays into the gamma-ray detector, which is required for radioxenon detection. This paper discusses the measurement details and provides recommendations for further research and optimization.

OBJECTIVE

The Automated Radioxenon Sampler/Analyzer (ARSA) system detects and measures the relative concentrations of radioxenon isotopes, seeking a definitive signature of nuclear explosions. A full description of the ARSA system is given elsewhere (Bowyer 1998), and only a brief synopsis will be given here. The system collects and processes air samples, filtering out particulates and unwanted elements. The xenon is separated and pumped into scintillating plastic cells for β detection, which are surrounded by NaI(Tl) γ-ray detectors. The radioxenon isotopes are detected by operating the β and γ-ray detectors in coincidence. Isotopic ratios of xenon can be determined by the signatures observed in the β-γ coincidence spectrum (Reeder 1998). Specific isotopic ratios indicate the occurrence of a nuclear explosion.

In ARSA field tests, a memory effect was observed wherein the β-γ coincidence system would measure latent radioactivity in the gas cells after they had been evacuated. Not all of the radioactivity could be pumped out of the system (McIntyre 2001). Corrections for this increased background were successfully applied, but the sensitivity of the system was poorer than what could be obtained if there were no memory effect.

The objective of this work is to test two possible methods for mitigating the memory effect in the gas cell used for detection of radioactive xenon. The first technique involves depositing a metal on the interior surface of the β cell, which should inhibit the adhesion of the gas to the cell walls and the diffusion of noble gases into the cell walls. The second method uses an inorganic, rather than plastic, scintillator to detect β radiation, which should have a similar effect as the metal. The experimental methods and results are discussed in the paper, and a recommendation is provided for future designs.

RESEARCH ACCOMPLISHED

Metallization Experiments

Aluminum, chrome, and copper were all tested as surface treatments for the scintillation cells. Al and Cu were evaporated at a rate of 9 Å/s onto the plastic under vacuum conditions using an electron-beam chamber at the Environmental Molecular Sciences Laboratory (EMSL) at PNNL. Chrome was deposited thermally in the same chamber. The total thickness of the metals was estimated to be roughly 1 μm in all cases. Shown in Figure 1 is a copper coated cell. The outside of the cell remains uncoated, as seen on the endcap in the figure.

The scintillation cells used in this experiment are not the original design for ARSA, which had cylindrically shaped scintillators with two photomultiplier tubes (PMTs) embedded in NaI(Tl) blocks. Cooper et al. present concurrently with this work the modifications—including the new bullet-shaped cell design—used to improve the reliability of ARSA system (Cooper 2005). In this experiment, the new cell design is used.

Figure 1. Photograph of copper-coated plastic scintillating gas cell and endcap for detection of β radiation. Only the interiors of the cell and endcap are metallized.

To test the light collection capability of the metallized cells, we examined the energy spectra from several γ-ray sources placed near the endcap. The endcap (by itself) was optically coupled to a photomultiplier tube, and both were placed inside a light-tight housing. γ-ray sources were placed individually against the outer wall of the housing, and the resulting energy spectra are recorded using an Ortec DART connected to a laptop computer. Due to the low atomic numbers of the elements present in the endcap, very little photoabsorption occurs in the scintillator. Almost all observed interactions are due to Compton scatter, which results in a continuum not unlike β energy spectra. The endpoints of these distributions are the Compton edges, which occur at a known energy for a given γ-ray energy.

Figure 2 shows the comparison between observed distribution endpoints and known Compton edge energies. The data follow a 2nd-order polynomial trend. For a thick detector, one would expect a linear trend between the energy of the scattered Compton electron and the observed channel number. However, higher energy electrons can escape from the β cell before losing all their energy. Therefore, for high-energy electrons the amplitudes of the pulses from the β cell are reduced compared to the amplitude corresponding to the full energy of the electron.

The chrome and copper data show a reduced channel number compared with the other endcaps, indicating less light collection. This is not surprising, given that the visible light reflectivities of chrome (~0.6) and copper (~0.4) are much smaller than that of aluminum (~0.95) (*CRC Handbook*). Thus, more light is reflected at the aluminum surface back into the scintillator for possible collection at the PMT than for the other metals. Additionally, copper specifically is a poor choice of metal not only for its selective frequency absorption characteristics (i.e. what gives copper its unique color) but also because it was easily peeled from the surface of the cell. During cell evacuation and filling, it is likely that some of the copper would flake off and cause a blockage in the gas transfer system. No such fragility was observed with the aluminized cell.

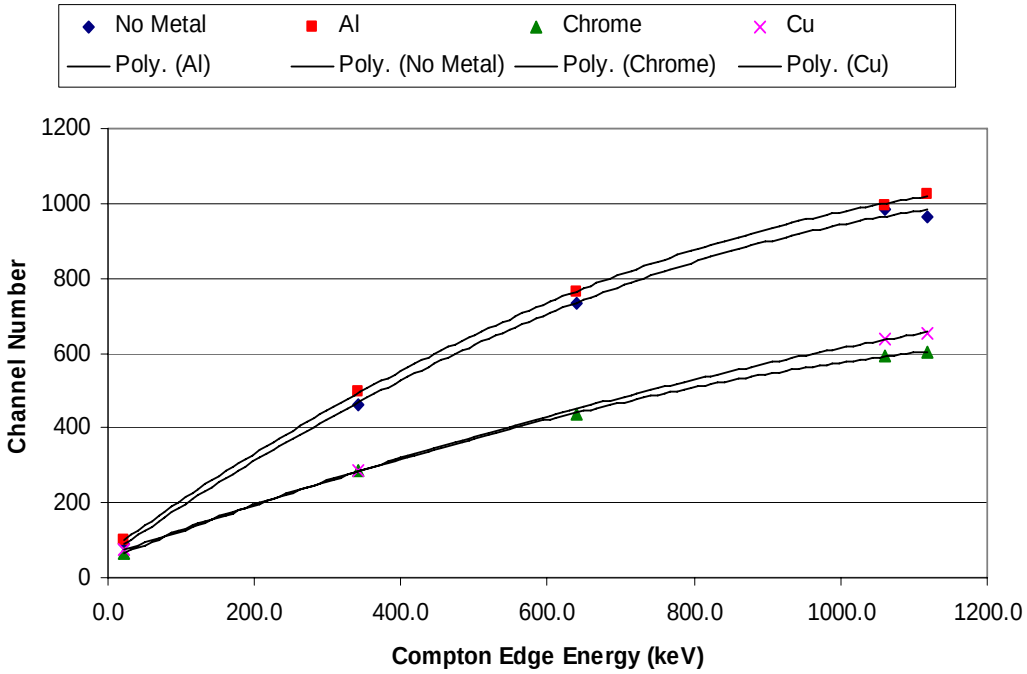

Figure 2. Comparison of observed Compton edge channel numbers with known energies for the different metallization schemes. The data follow 2nd-order polynomials.

The aluminum and bare cells were then fully assembled and sealed with optical cement. The cells were wrapped in Teflon tape to improve light collection efficiency, were coupled to a PMT, and were again placed inside a light-tight housing. The γ-ray measurements were repeated for the two cells, and the results are given in Figure 3. Again the performance of the aluminum coated cell was similar to that of the bare cell, except that the light output was slightly higher. The total light output of the fully assembled cells was about twice that of the endcaps alone. The γ-ray measurements demonstrate that aluminum is a good choice for metallization and does not result in any loss of signal in the β cell.

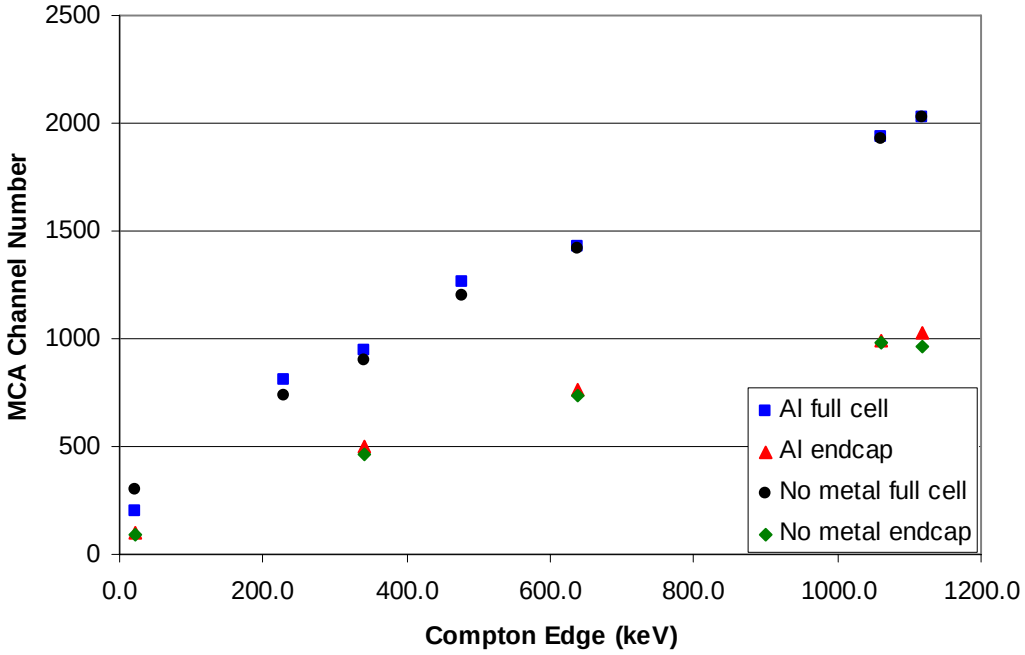

Figure 3. Comparison of observed Compton edge channel numbers with known energies for the endcaps and fully assembled bare and aluminum-coated cells.

Radioactive Xenon Measurements

To test the memory effect of the scintillations cells, radioactive gas measurements were performed. The bare plastic cell and aluminum-coated plastic cell were tested along with an inorganic scintillator cell composed of yttrium aluminum perovskite (YAP). Stainless steel gas tubes were inserted into the cells and secured in place with optical cement and then opaque epoxy. The β cell housings were placed in the void of a CsI(Na) well detector, and the assembly was encased in black polyethylene. The detectors were placed in a 4-inch-thick lead cave with a 0.25-inch-thick copper lining to reduce ambient background from cosmogenic and environmental radioactive sources.

Radiation measurements were taken before, during, and after exposure to radioactive gases in the following manner. The cells were evacuated using a vacuum pump, typically resulting in pressures of a few mTorr. Background data were taken for 24 hours. Because the cells tend to leak up to atmospheric pressure over the course of one day, they were again pumped to low pressures before the radioactive gas was injected. Again, data were taken for 24 hours. The cell was then pumped and flushed with ambient air three times before a final 24-hour background measurement was performed. This procedure was used for both radioxenon and radon measurements.

Figure 4 shows the 2-D β-γ coincidence spectrum for the bare cell injected with radioxenon. There are two main γ-ray peaks, corresponding to the 81 keV γ ray from Xe-133g and 30 keV x-ray emitted from all xenon isotopes. The β spectrum is the sum of contributions of the electron energies from Xe-131 (129 keV conversion electron (CE)), Xe-133m (199 keV CE), and Xe-133g (346 keV max β energy). A detailed discussion of this spectrum is provided by Reeder (Reeder et al. 1998).

If the β cells exhibited no memory effect, then the count rate after pumping the gas out of the cell should be the same as that in the background measurement before gas injection. Two xenon regions, shown in Figure 4, are defined, and the count rates in each region are compared with and without the gas present. The count rates are corrected for the observed background. The results for each detector type are given in Table 1. The bare cell demonstrated a very large count rate even after the cell was evacuated. Previous estimates of the memory effect were about 5% for a bare cell with radioxenon (McIntyre 2001), and the observed rates may be artificially high due to a malfunctioning vacuum pump.

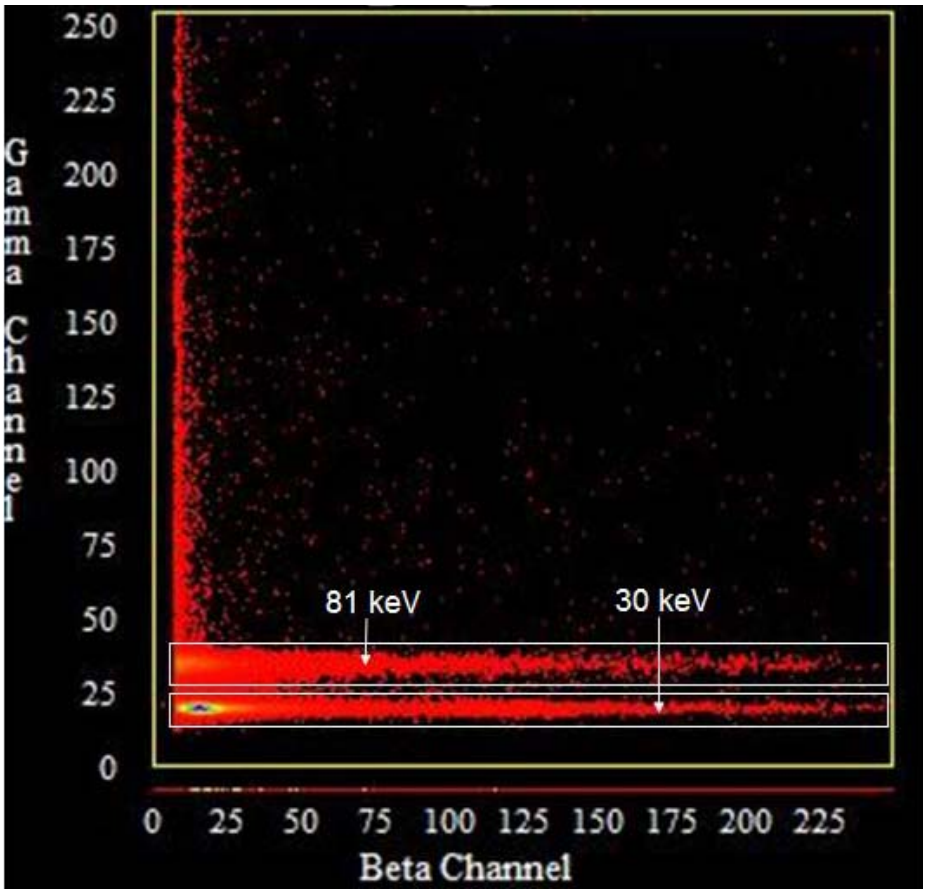

Figure 4. β-γ coincidence spectrum for aluminum-coated cell injected with radioxenon. Rectangular "xenon regions" are defined for further quantitative evaluation.

Table 1. Percent of Xenon Count Rates Observed after Evacuation of Gas Cell in 30 keV and 81 keV Regions of Xenon β-γ Coincidence Spectrum

	30 keV	81 keV
Bare	94 ± 4 %	80 ± 7%
Aluminized	7.8 ± 0.2%	8.1 ± 0.4%
YAP	Not observed	8 ± 2%

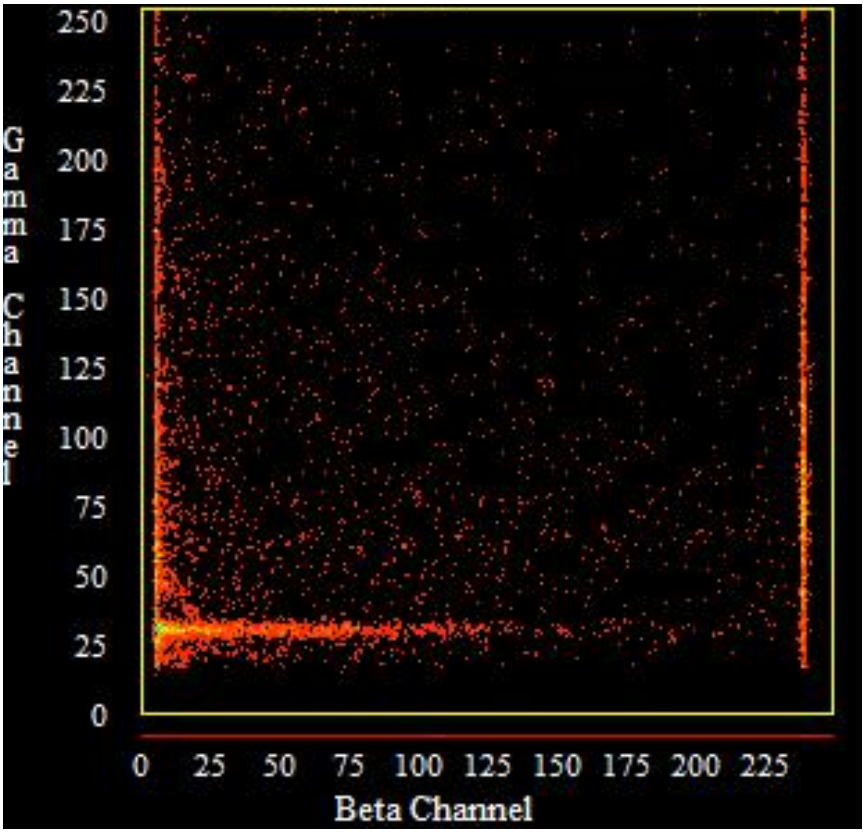

Figure 5. β-γ coincidence spectrum for YAP cell injected with radioxenon. Only the 81 keV γ-ray peak is visible in the spectrum.

It is important to note that the β-γ coincidence spectrum for the YAP cell consists of only one γ-ray peak, as seen in Figure 5. Because the YAP cell has a much higher effective atomic number than the plastic scintillator, the 30-keV x-rays from Xe are more likely to be absorbed in the β cell directly and will not reach the CsI(Na) detector to initiate a coincidence. Also visible in Figure 5 is a bright line corresponding to high β energies; this is actually overflow in the multi-channel analyzer. The high-energy electrons that enter the cell walls from the gas deposit more of their energy in the YAP cell than in the plastic cell due to the higher stopping power of YAP. The analyzer puts these high-energy counts in the last few β channels. In addition, despite the calculated 8±2% effect shown in Table 1, the γ-ray spectrum shows very little evidence of latent radioactivity, as seen in Figure 6. There is an elevated background shelf, but no evidence of a peak in the 81-keV vicinity. This is unlike the aluminized cell, for which two small peaks are visible in the γ-ray spectrum data taken after the cell was evaculated (not shown).

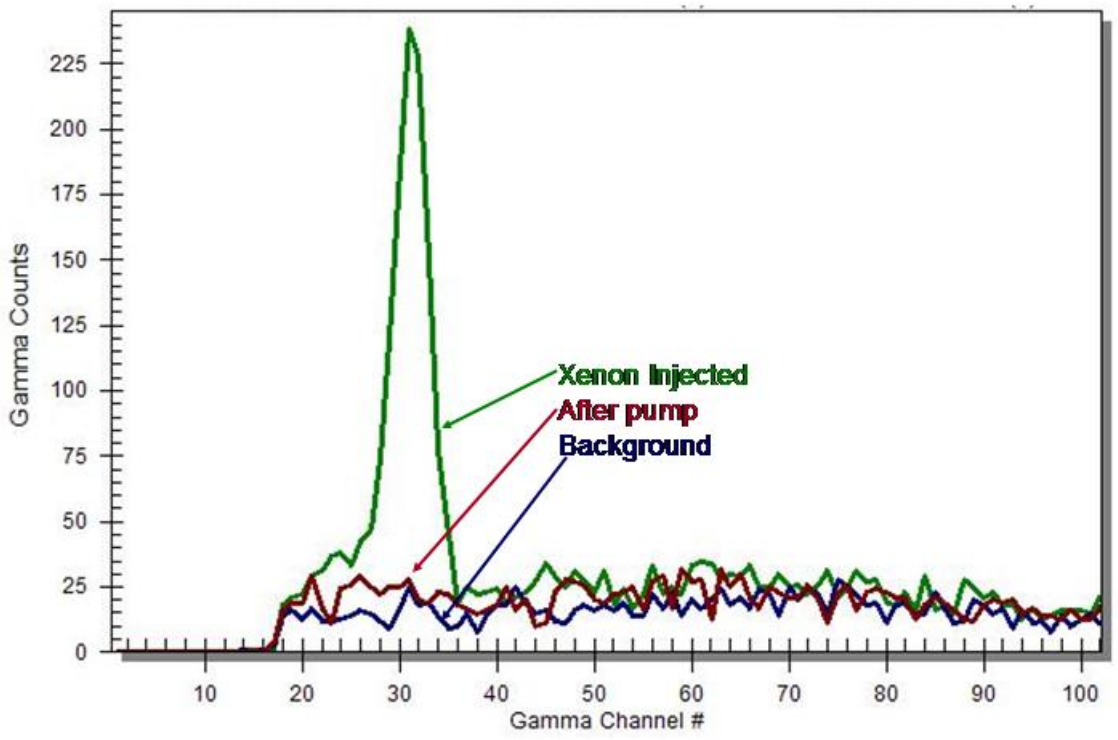

Figure 6. β-gated γ-ray spectrum using YAP cell with xenon injected.

Radioactive Radon Measurements

The ARSA system is designed to measure radioxenon, and the presence of radon isotopes can be detrimental. The atmospheric concentration of ^{222}Rn is ~ 10 Bq/m^3, which is 10^5 times greater than the desired sensitivity level of ^{133}Xe in the ARSA system (Bowyer 1998). Furthermore, not all of the ^{222}Rn is filtered from the air in the gas separations process—only about 99.98% of the radon is removed (McIntyre 2001). In terms of the memory effect, the influence of radon is significant. Unlike the Xe isotopes, which decay to stable or long-lived nuclides, the Rn daughters have very short half-lives (on the order of seconds or minutes), and thus have a relatively high activity. Because the Rn daughters are not noble gases, they are likely to adhere to the cell walls and not be pumped out of the cell, which leads to a higher latent activity from radioactive contaminants in the cells after evacuation than if the sample consisted only of xenon. This was confirmed by previous measurements: the memory effect for radon is larger than that for xenon (McIntyre 2001). With the β-γ coincidence method, simply having extra radioactivity would not in itself be detrimental. However, ^{222}Rn decays to ^{214}Pb and ^{214}Bi, which have γ- and x-rays that interfere with the 81 keV and 250 keV γ rays from ^{133g}Xe and ^{135g}Xe, respectively.

In the past, corrections have been made to account for the memory effect due to the radon impurities in the gas (McIntyre 2001). A system in which there is no memory effect for radon—or at least reduces the magnitude of such an effect—would result in a higher sensitivity for radioxenon. Thus, we performed the radioactive gas experiments using radon on each of the three detector types to measure the improvement, if any, compared with the bare cell.

Shown in Figure 7 is the β-γ coincidence spectrum for the bare cell. There are several γ-ray energies observed in coincidence with β or CEs from the radon daughters. These correspond to the 352 keV, 295 keV, and 242 keV γ-rays from ^{214}Pb, as well as x-rays from ^{214}Pb and ^{214}Bi between 75 to 90 keV. Figure 8 shows a comparison of the β-gated γ-ray spectra for radon and xenon for the bare cell. The interference at 81 keV is clearly seen.

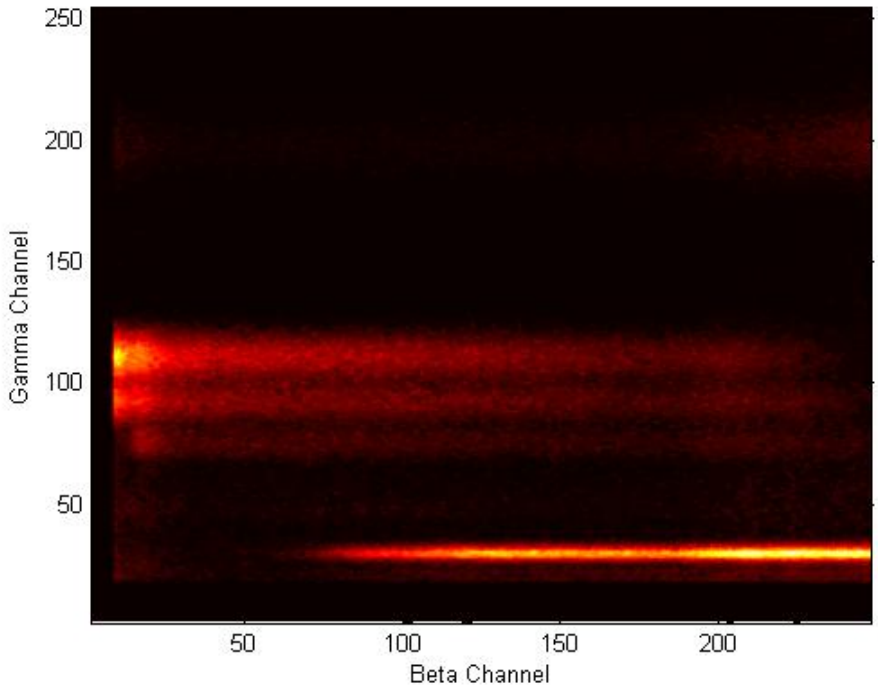

Figure 7. β-γ coincidence spectrum for bare cell injected with radon.

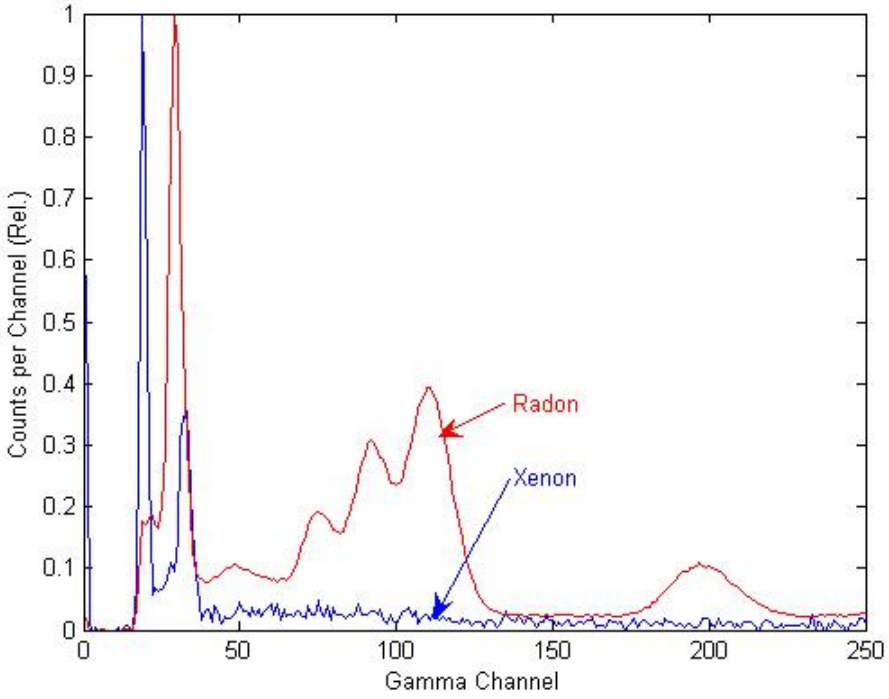

Figure 8. Normalized β-gated γ-ray spectra for radon and xenon injection in a bare cell. Note the overlap in signatures at 81 keV (γ channel 34).

For the radon measurements, the comparison of the total count rate before and after the radon-filled cell is evacuated is used as a measure of the memory effect. Corrections must be made in the count rates to account for the decay of ^{222}Rn (half-life of 3.8 days) during the two 24-hour measurements. Consider the following. The number of counts C observed between times t_1 and t_2 for a source with activity $A(t)$ is given by

$$C = \varepsilon \int_{t_1}^{t_2} A(t)dt \,, \tag{1}$$

for a constant detection efficiency ε. The main contribution of the ^{222}Rn chain to the β-γ coincidence spectrum will be from ^{214}Pb and ^{214}Bi. The radionuclides in the chain that alpha decay do not produce a coincidence signature in the detectors, and the ^{214}Bi daughter, ^{214}Po quickly alpha decays to ^{210}Pb, which has a half-life (23 years) that is long compared to the acquisition time. Thus,

$$C = \varepsilon \int_{t_1}^{t_2} \left[A_{Pb}(t) + A_{Bi}(t)\right]dt \,. \tag{2}$$

The activities $A_{Pb}(t)$ and $A_{Bi}(t)$ can be calculated using the Bateman equation for radioactive decay. Furthermore, the activities are directly proportional to the amount of radon present at $t=0$, $N_{Rn}(0)$:

$$A_i(t) = N_{Rn}(0)\, f_i(t) \,, \tag{3}$$

where i indicates ^{214}Pb or ^{214}Bi. Therefore, the initial amount of radon can be estimated from the observed count rates, estimated detection efficiency, and decay functions $f_i(t)$:

$$N_{Rn}(0) = \left[\frac{C}{\varepsilon \int_{t_1}^{t_2} \left[f_{Pb}(t) + f_{Bi}(t)\right]dt} \right]. \tag{4}$$

The estimated amount of radon at $t=0$ is calculated for the data collected before and after the evacuation of the cell. The ratio of the two estimates yields a measure of the radon remaining in the cell after evacuation, and thus is a measure of the memory effect. Because ratios of the radon estimates are used, the detector efficiency term cancels.

The integrand in the equations above, dubbed the "total effective activity", is shown in Figure 9. Also plotted in Figure 9 is the evaluated integral for $t_1=0$ and t_2 plotted on the horizontal axis. This is the effective number of disintegrations that have occurred until t_2. The vertical scales on both graphs are relative; the use of ratios allows us to neglect the absolute value of these functions.

To appropriately correct the data, the measured counts are first background subtracted to yield the measured counts C. Then, Equation (4) is evaluated (neglecting the efficiency term) using the number of disintegrations function in Figure 9, and the estimated initial amounts of radon are determined. The ratio of radon estimates after and before evacuation is calculated for each detector type, and the results are given in Table 2.

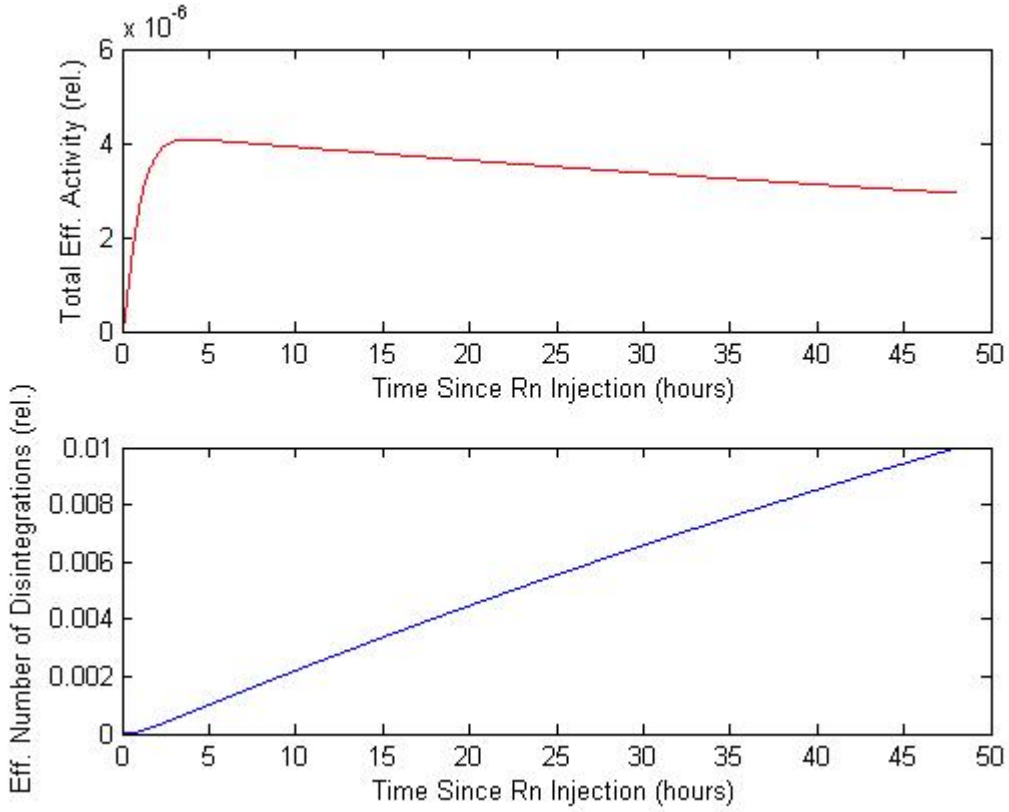

Figure 9. a) Total effective activity—the sum of ^{214}Bi and ^{214}Pb activities as a function of time after ^{222}Rn injection. b) Effective number of disintegrations from ^{214}Pb and ^{214}Bi as a function of time after injection.

Table 2. Memory Effect Estimates for Radon-Injected Gas Cells

	Memory Effect
Bare	19.6%
Aluminized	13.5%
YAP	1.8%

The estimated effect for the bare cell was approximately 20%, which is similar to numbers previously reported for the ARSA system and is much less than determined in this work for Xe. This indicates a possible vacuum pump malfunction during the xenon experiments. Actual cell pressures were not monitored during every experiment. The aluminized cell showed an increase in the memory effect for radon compared with xenon, as expected. Also, the aluminum coating on the cell did have the desired effect—there was an observed reduction in latent activity relative to the bare cell for radon. The YAP cell demonstrated surprisingly good performance in the radon experiment. Very little radon was observed in the cell after the experiment.

There were a few strange features observed in the data. The acquisition software is capable of tracking the count rates as a function of time. There was an initial coincidence count rate decrease due to the decay of the radon daughters that remained in the cell after evacuation. This is expected. However, later, in both the aluminized and

bare cells, there were anomalous changes in the count rate that cannot be accounted for. The rates were not measured for the YAP cell. These same features exist also for the β singles and γ singles count rates. It is unclear what caused these rate changes or if they affect the spectroscopic data in the β-γ coincidence spectrum. Further measurements are required to determine the cause of this behavior.

CONCLUSIONS AND RECOMMENDATIONS

The radon data clearly demonstrate that using an inorganic surface on the β cell reduces the memory effect from gases remaining in the cells after evacuation. Depositing aluminum on the surface of the plastic cell reduced the memory effect from 20% to 14%. This could lead to better ARSA performance. The YAP cell performed extremely well in both the xenon and radon measurements. With additional optimization of the cell wall thickness (less than 2mm) the YAP cell will provide excellent beta detection while allowing the low energy x-rays to pass through for detection in the surrounding NaI(Tl). In addition, the present configuration of the YAP cell may be more appropriate as a β detector when higher energy γ rays are detected, such as with radon.

While not discussed in this paper, the energy resolution of the YAP is far superior to the energy resolution of the plastic. Additional testing using a thin walled YAP cell will be able to exploit this energy resolution in detecting the 129-keV and 199-keV conversion electron energies of ^{131m}Xe and ^{133m}Xe respectively. Additional studies are continuing on the three cells considered in this paper and a thin walled version of the YAP cell will be available during FY 06 to investigate both the x-ray attenuation issue and the enhanced energy resolution properties.

REFERENCES

Bowyer, T.W., K.H. Abel, C.W. Hubbard, A.D. McKinnon, M.E. Panisko, R.W. Perkins, P.L. Reeder, R.C. Thompson, and R.A. Warner (1998). Automated separation and measurement of radioxenon for the Comprehensive Test Ban Treaty, *Journal of Radioanalytical and Nuclear Chemistry*, 235: 1-2: 77–81.

Cooper, M.W., A. J. Carman, J.C. Hayes, T.R. Heimbigner, C.W. Hubbard, K.E. Litke, J.I. McIntyre, S.J. Morris, M.D. Ripplinger, and R. Suarez (2005), Improved β-χ coincidence detector for radio-xenon detection, in current Proceedings.

CRC Handbook of Chemistry and Physics, Editor D.R. Lide (2001), 12: 153.

McIntyre, J. I., K. H. Abel, T. W. Bowyer, J. C. Hayes, T. R. Heimbigner, M. E. Panisko,P. L. Reeder, R. C. Thompson (2001), Measurements of Ambient Radioxenon levels using the Automated Radioxenon Sampler/Analyzer (ARSA), *Journal of Radioanalytical and Nuclear Chemistry*, 248: 3, 629–635.

Reeder, P.L., and T.W. Bowyer (1998), Xe isotope detection and discrimination using beta spectroscopy with coincident gamma spectroscopy, *Nuclear Instruments and Methods in Physics Research*, A408: 582–590.